Mitochondrial delivery of Coenzyme Q_{10} *via* systemic administration using a MITO-Porter prevents ischemia/reperfusion injury in the mouse liver

Yuma Yamada[a,e], Kohei Nakamura[a,e], Jiro Abe[a,b], Mamaru Hyodo[c], Sanae Haga[d], Michitaka Ozaki[d], Hideyoshi Harashima[a,*]

[a] Laboratory for Molecular Design of Pharmaceutics, Faculty of Pharmaceutical Sciences, Hokkaido University, Sapporo, Japan

[b] Department of Pediatrics, Hokkaido University Hospital, Kita-15, Nishi-7, Kita-ku, Sapporo 060-8638, Japan

[c] Faculty of Engineering, Department of Applied Chemistry, Aichi Institute of Technology, Toyota, Japan

[d] Laboratory of Molecular and Functional Bio-Imaging, Faculty of Health Sciences, Hokkaido University, Sapporo, Japan.

[e] These authors contributed equally as first author

*To whom correspondence should be addressed:

Tel +81-11-706-3919 Fax +81-11-706-4879 E-mail harasima@pharm.hokudai.ac.jp

Abstract

We herein report on a mitochondrial therapeutic effect based on the delivery of coenzyme Q_{10} (CoQ_{10}), an anti-oxidant, to *in vivo* mitochondria using a MITO-Porter, a liposome-based mitochondrial delivery system that functions *via* membrane fusion. To evaluate the effects, we used a mouse liver ischemia/reperfusion injury (I/R injury) model, in which mitochondrial reactive oxygen species are overexpressed. We packaged CoQ_{10} in the lipid phase of a MITO-Porter and optimized the mitochondrial fusogenic activities to produce the CoQ_{10}-MITO-Porter. A histological observation of the carriers in the liver by confocal laser scanning microscopy was done and the accumulation of the carrier labeled with a radio isotope in the liver confirmed that the CoQ_{10}-MITO-Porter was delivered to liver mitochondria *via* systemic injection. These analytical results permitted us to optimize the compositions of the CoQ_{10}-MITO-Porter so as to permit it to efficiently accumulate in mouse liver mitochondria. Finally, we applied the optimized CoQ_{10}-MITO-Porter to mice *via* tail vein injection, and hepatic I/R injury was then induced, followed by measuring serum alanine aminotransferase (ALT) levels, a marker of liver injury. We confirmed that the use of the CoQ_{10}-MITO-Porter resulted in a significant decrease in serum ALT levels, indicating that *in vivo* mitochondrial delivery of the CoQ_{10} *via* MITO-Porter prevents I/R injury in mice livers. This provides a demonstration of the potential use of such a delivery system in mitochondrial therapies.

Keywords: Mitochondria; mitochondrial delivery; antioxidant chemicals; coenzyme Q_{10}; ischemia/reperfusion injury; MITO-Porter; *in vivo* delivery.

Abbreviations

[^{3}H]-CHE, ^{3}H-Cholesterylhexadecyl ether; ALT, alanine aminotransferase; AST, aspartate aminotransferase; Ch, channel; CLSM, confocal laser scanning microscopy; COX IV, cytochrome c oxidase subunit IV; DiI, 1,1′-dioctadecyl-3,3,3′,3′-tetramethylindocarbocyanine perchlorate; DMG-PEG 2000, 1,2-dimyristoyl-sn-glycerol, methoxypolyethylene glycol 2000; DOPE, 1,2-dioleoyl-sn-glycero-3-phosphatidyl ethanolamine; EPC, egg yolk phosphatidylcholine; CoQ_{10}, coenzyme Q_{10}; GAPDH, Glyceraldehyde 3-phosphate dehydrogenase; GS-IB4-FITC, fluorescein isothiocyanate-conjugated griffonia simplicifolia isolectin B4; HEPES, 4-(2-hydroxyethyl)-1-piperazineethanesulfonic acid; I/R injury, ischemia/reperfusion injury; MIB, mitochondrial isolation buffer; NBD-DOPE, 7-nitrobenz-2-oxa-1,3-diazole labeled DOPE; PBS (-), phosphate-buffered saline; RI, radio isotope; ROS, reactive oxygen species; SM, sphingomyelin; STR-R8, stearylated octaarginine.

1. Introduction

In recent years, various mitochondrial dysfunctions have been implicated in a variety of diseases [1-3]. Thus, research and development directed toward mitochondrial medicine would be expected to have great medical benefits to society in general. Thus, researchers dealing with mitochondrial drug delivery systems are encouraged to develop such therapeutic strategies based on the *in vivo* mitochondrial delivery of therapeutics. Various types of mitochondrial delivery systems have been reported during the past decades [4-8], but only a limited number of these approaches have the potential for use in mitochondrial therapy. These strategies face many problems including cell internalization, size limitations and the physicochemical properties of the cargo, modification of a functional device and the denaturation of the cargo [5, 9, 10].

We previously reported on the construction of a MITO-Porter, a liposome-based mitochondrial delivery system that functions *via* membrane fusion [5, 11]. This membrane fusion mechanism-based strategy can deliver a cargo to mitochondria independent of its size and physical properties. To date, we have shown that the MITO-Porter can be used to deliver a variety of therapeutic cargoes, including an anti-apoptosis chemical and an anti-oxidant chemical, to the mitochondria of human cells [12, 13]. As a result, the mitochondrial delivery of therapeutic cargoes have potential for functioning as a mitochondrial therapeutic strategy, indicating that the MITO-Porter represents a potentially useful carrier for use in mitochondrial medicine, based on *in vitro* experiments.

The purpose of this study was to validate the utility of the mitochondrial therapeutic strategy by targeting *in vivo* mitochondria as shown in Figure 1. The schematic image indicates the antioxidant effect conferred by delivering coenzyme Q_{10} (CoQ_{10}), an anti-oxidant, to liver mitochondria in a mouse ischemia/reperfusion injury (I/R injury) model, using the MITO-Porter. Under an ideal scenario, the MITO-Porter encapsulating CoQ_{10} reaches the liver tissue *via* systemic injection, and the carrier is then internalized into hepatocytes *via* macropinocytosis. In the cytosol, the carrier delivers CoQ_{10} to mitochondria *via* membrane fusion, resulting in the creation of a pharmacological effect of CoQ_{10} in mitochondria. Reactive oxygen species

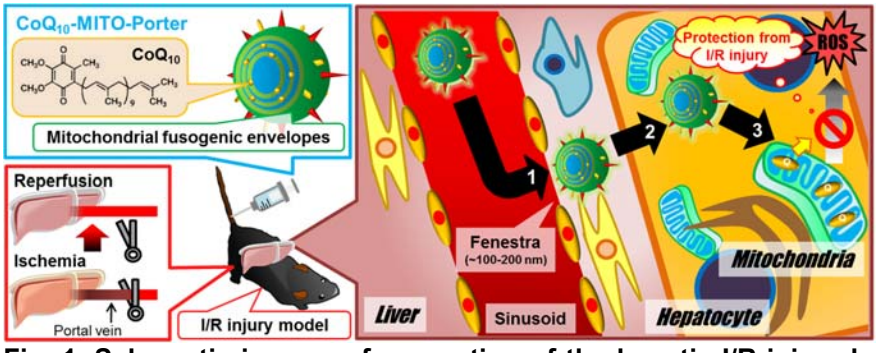

Fig. 1. Schematic images of prevention of the hepatic I/R injury by mitochondrial delivery of CoQ_{10} using MITO-Porter system. CoQ_{10}, coenzyme Q_{10}; I/R, ischemia/reperfusion; ROS, reactive oxygen species.

(ROS) are mainly produced in the mitochondrial respiratory chain, and are associated with a variety of diseases including I/R injury, neurodegenerative diseases, tumor metastasis, metabolic syndrome and aging [5, 14-18]. Thus, a therapeutic strategy for the mitochondrial delivery of antioxidant chemicals could be useful for the treatment of these diseases. To evaluate the anti-oxidant effects resulting from the mitochondrial delivery of CoQ_{10}, we used hepatic I/R injury induced mice that overexpress mitochondrial ROS in the liver. In such a situation, serum alanine aminotransferase (ALT) levels would be increased.

In this study, we prepared the CoQ_{10}-MITO-Porter by the ethanol dilution method, in which CoQ_{10} is contained in the lipid envelopes of the MITO-Porter, and attempted appropriately adjust the size of the particles. We also investigated the effect of the size of the CoQ_{10}-MITO-Porter on the distribution of the carrier in liver tissue post systemic injection by histological observations using confocal laser scanning microscopy (CLSM). A knowledge of the extent of mitochondrial binding and the fusogenic activities of the CoQ_{10}-MITO-Porter permitted us to determine the optimal composition for the constructing a CoQ_{10}-MITO-Porter with a high mitochondrial fusogenic activity. Histological observations by CLSM and the use of a carrier labeled with a radio isotope (RI) verified that the CoQ_{10}-MITO-Porter was delivered liver mitochondria *via* systemic injection. Finally, we injected mice with the optimized CoQ_{10}-MITO-Porter *via* the tail vein, and hepatic I/R injury was then induced, followed by measurements of serum ALT levels, a marker of liver injury.

2. **Materials and methods**

2.1. Materials

1, 2-dioleoyl-sn-glycero-3-phosphatidylethanolamine (DOPE), egg yolk phosphatidyl choline (EPC), sphingomyelin (SM), 7-nitrobenz-2-oxa-1,3-diazole labeled DOPE (NBD-DOPE) and rhodamine-DOPE were purchased from Avanti Polar lipids (Alabaster, AL, USA). 1,2-dimyristoyl-sn-glycerol, methoxypolyethylene glycol 2000 (DMG-PEG 2000) was obtained from the NOF Corporation (Tokyo, Japan). Stearylated octaarginine (STR-R8)[19] was obtained from Kurabo Industries Ltd (Osaka, Japan). CoQ_{10} was obtained from Wako Pure Chemical Industries, Ltd. (Osaka, Japan). ^{3}H-Cholesterylhexadecyl ether ([^{3}H]-CHE) was purchased from PerkinElmer Life Science (Waltham, MA, USA). 1,1′-dioctadecyl-3,3,3′,3′-tetramethylindocarbocyanine perchlorate (DiI) was purchased from Invitrogen Corp (Carlsbad, CA, USA). Hoechst33342 was purchased from DOJINDO Laboratories (Kumamoto, Japan). Fluorescein isothiocyanate-conjugated griffonia simplicifolia isolectin B4 (GS-

IB4-FITC) was purchased from Vector Laboratories Inc. (Stuttgart, Germany). MitoQ was synthesized as described in a previous report [20], and the chemical structure is shown in Figure S2A. Mitochondria were isolated from mouse liver essentially, as described in Supplementary material. All other chemicals used were commercially available reagent-grade products.

2.2. Experimental animals

C57BL/6 male mice (6 weeks old) were purchased from Japan SLC (Shizuoka, Japan). All animal protocols were approved by the institutional animal care and research advisory committee at the Faculty of Pharmaceutical Sciences, Hokkaido University, Sapporo, Japan (date: 22 March 2013, registration no. 13-0062).

2.3. Preparation of MITO-Porter and PEG-LP by lipid hydration method.

The lipid film for the MITO-Porter was produced on the bottom of a glass tube by the evaporation of a chloroform/ethanol solution containing 137.5 nmol lipids (DOPE/SM = 9:2, molar ratio). After the formation of the film, 250 μL of 10 mM 4-(2-hydroxyethyl)-1-piperazineethanesulfonic acid (HEPES) buffer (pH 7.4) was added, followed by incubation for 15 min at room temperature and sonication for 1 min in a bath-type sonicator (85W, Aiwa, Co., Tokyo, Japan). To attach R8 to the surface of the carrier, a solution of STR-R8 (10 mol% of total lipids) was added to the resulting suspensions, followed by incubation for 30 min at room temperature. In preparation of PEG-LP, the lipid film composed of DOPE/SM/DMG-PEG2000 (9/2/0.33, molar ratio) was used. The lipid compositions of these carriers are summarized in Table S1. For histological observation shown in Figure 2A, the carriers were labeled with DiI (0.5 mol% of total lipids). For investigation of liver accumulation shown in Figure 2C, the carriers were labeled with [^{3}H]-CHE (0.023 mol% of total lipids).

2.4. Construction of carriers by the ethanol dilution method.

To evaluate the hepatoprotective effect from I/R injury (Figures 5, 6), carriers containing CoQ_{10} were constructed by the ethanol dilution method by the following 4 steps as shown in Figure 3A. A 100% (v/v) EtOH solution containing 5.5 mM lipids [DOPE(or EPC)/SM/DMG-PEG2000 (9/2/0.33, molar ratio)] with/without CoQ_{10} (18 mol% of lipids) were prepared. The lipid in the EtOH solution was mixed with phosphate buffered saline (PBS (-)) under strong agitation to a concentration of 90% (v/v)

EtOH (or 50% (v/v) EtOH for large sized CoQ_{10}-MITO-Porter) (1). The resulting suspension was then added to the PBS (-) under strong agitation to a final concentration of ~5% (v/v) EtOH (2). The ethanol was removed by ultrafiltration through an Amicon system (MWCO 100,000; Millipore, Billerica, MA, USA), and the external buffer replaced with PBS (-) (3). To attach R8 to the surface of the carrier, a solution of STR-R8 (3 or 10 mol% lipids) was added to the resulting suspensions, followed by incubation for 30 min at room temperature (4). The lipid compositions of these carriers are shown in Tables 1-3 and Table S2.

For histological observation shown in Figures 3B, 4C, a HEPES buffer was used to prepare the carriers containing a lipid film labeled with DiI (0.5 mol% of total lipids). For the mitochondrial binding assay (Figures 4A, 6A), the carriers containing a lipid film labeled with 1 mol% NBD-DOPE were prepared with mitochondrial isolation buffer [MIB (-): 250mM sucrose, 2 mMTris–HCl, pH 7.4]. To investigate mitochondrial fusogenic activity (Figures 4B, 6A), dual-labeled carriers containing both 1 mol% NBD-DOPE and 0.5 mol% rhodamine-DOPE were prepared with MIB (-). For investigation of liver accumulation shown in Figure 2C, the carriers labeled with [^{3}H]-CHE (0.019 mol% of total lipids) were prepared with HEPES buffer.

2.5. Characterization of carriers.

Particle diameters were measured using a dynamic light scattering method (Zetasizer Nano ZS; Malvern Instruments, Worcestershire, UK). The values of particle diameters are shown in the form of volume distribution. The ζ-potentials of samples were also determined in 10 mM HEPES buffer using a Zetasizer Nano ZS. Encapsulation efficiency of the CoQ_{10} into MITO-Porter was estimated, as described in the Supplementary material.

2.6. Mitochondrial binding activity using isolated mitochondria.

The mitochondrial binding activity of the carrier was determined by fluorescence measurements. A 270 μL aliquot of suspension of isolated mouse liver mitochondria (1 mg protein/mL) and a 30 μL aliquot of NBD labeled liposome (lipid concentration 0.55 mM) were mixed and incubated for 30 min at 25°C. A 150μL aliquot of the resulting solution was mixed with 150 μL of EDTA-free MIB containing triton (final concentration, 0.25% (v/v)), denoted as sample A. The remaining suspension was centrifuged (8,000 *g*, 10 min, 4 °C), and washed with EDTA-free MIB and re-precipitated by centrifugation (8,000 *g*, 10 min, 4 °C). The pellet was resuspended in 300 μL EDTA-free MIB

containing 0.25% (v/v) triton, to give sample B. The fluorescence intensities of Samples A and B were measured with excitation at 470 nm and emission at 530 nm (EnSpireTM 2300 Multilabel Reader; PerkinElmer Inc. Waltham, MA, USA).

Mitochondrial binding activity was calculated as follows:

Mitochondrial binding activity (%) = $F_B/F_A \times 100$

where F_A and F_B represent the fluorescence intensity of sample A and B.

2.7. Membrane fusion assay using FRET analysis

The fusion activity of the carriers with isolated mitochondrial membranes was assessed by FRET as previously described [9, 11, 21]. In this experiment, lipid envelopes of the dual-labeled carriers were labeled with both NBD (excitation at 460 nm and emission at 534 nm) and rhodamine (excitation at 550 nm and emission at 590 nm) so that the energy would be transferred from NBD to rhodamine. A 10-μL aliquot of dual-labeled carriers (lipid concentration, 0.55 mM) was added to a suspension of isolated mouse liver mitochondria (1 mg of protein / mL) in 90 μL of MIB (-EDTA), and incubated for 30 min at 25ºC. After the incubation, energy transfer was assessed by measuring the fluorescent intensity (excitation at 470 nm and emission at 530 nm) using an EnSpireTM 2300 Multilabel Reader. The maximum fluorescence was defined as the fluorescence of the liposomes when dissolved in Triton X-100 (final concentration, 0.5% (v/v)). Fusion activity (%) was estimated by the reduction in the level of energy transfer in accordance with membrane fusion, and was calculated as follows:

Fusion activity (%) $=(F - F_0)/(F_{max} - F_0) \times 100$

where F, F_0 and F_{max} represent the fluorescence intensity of labeled carrier after incubation with mitochondria, the fluorescence intensity of labeled carrier after incubation without mitochondria, and the maximum fluorescence intensity after the Triton X-100 treatment, respectively.

2.8. Histological observation for distribution of the carrier in liver tissue.

For the histological observation of carriers in the liver, carriers labeled with DiI were intravenously administered to mice *via* the tail vein at a dose of 2.75-7.0 μmol/kg of lipids in a total volume of 10 mL/kg. At 1-hr after the administration, each animal was perfused with saline containing heparin (40 U/mL) to remove blood from the liver, which was then collected and washed once with saline and once with Hank's balanced salt solution. The liver was sectioned into 1 mm thick sections, and incubated for

30 min in HEPES buffer containing Hoechst 33342 (final concentration, 40 μg/mL) to stain the nuclei, GS-IB4-FITC (final concentration, 40 μg/mL) to stain blood vessels, followed by obtaining fluorescent images by CLSM (Nikon A1; Nikon Co. Ltd., Tokyo, Japan). The tissue specimens were excited with a 405 nm wavelength light from a Diode laser, 488 nm wavelength light from an Ar laser and 561 nm wavelength light from a DPSS laser. A series of images were obtained using a Nikon A1 confocal imaging system equipped with a water immersion objective lens (Plan Apo 60_1.20 PFS WI) and a 1st dichroic mirror (405/488/561/640). The three fluorescence detection channels (Ch) were set to the following filters: Ch1: 450/50 (blue color) for nuclei stained by Hoechst 33342, Ch2: 525/50 (green color) for blood vessels stained by GS-IB4-FITC, Ch3: 595/50 (red color) for carriers labeled with DiI.

2.9. Quantification of carrier accumulation in liver mitochondria by RI.

To quantify the amounts of carrier that had accumulated in liver mitochondria, carriers labeled with [^{3}H]-CHE were intravenously administered to mice *via* the tail vein at a dose of 2.75 μmol/kg lipids in a total volume of 10 mL/kg. At 1-hr after the administration, each animal was perfused with saline containing heparin (40 U/mL) to remove blood from the liver, which was then collected and washed with saline. All subsequent steps were carried out on ice. After removing them from the saline, the livers were placed in 3 mL of ice-cold MIB, and were then minced with scissors and ice-cold MIB was added to give a total volume of 9 mL. The suspension was homogenized in a glass homogenizer (30 mL capacity) with a pestle using 3 complete up and down cycles (~ 550 rpm). A portion of the resulting homogenate was denoted as the liver homogenate sample. The remaining homogenate was mixed with approximately 1 mL of MIB and centrifuged at 800*g* for 5 min. The supernatant was transferred to ice-cold tubes and centrifuged at 7,500*g* for 10 min. The pellets were washed twice with EDTA-free MIB and reprecipitated by centrifugation (16,000*g*, 10 min). The resulting pellets were resuspended with EDTA-free MIB and the resulting suspensions were used as the mitochondria-enriched fraction. The purity of mitochondria-enriched fraction was confirmed by Western blotting to detect organelle specific proteins: Cytochrome c oxidase subunit IV (COX IV), mitochondrial specific protein; Histone H3, nuclear specific protein; Glyceraldehyde 3-phosphate dehydrogenase (GAPDH), cytosolic specific protein (see supplementary material for details). The protein concentrations of the liver homogenate and mitochondrial proteins were determined using a BCA protein assay kit (Pierce, Rockford, IL). The liver homogenate sample and the mitochondria-enriched fraction were lysed in Soluene-350 (Perkin Elmer) at 50°C over night, and 10 mL of Hionic Fluor (PerkinElmer) was added to lysate. RI counts of these samples were measured using an LSC-6100 (ALOKA, Tokyo, Japan). Liver accumulation and mitochondrial targeting activity were calculated as follows:

Liver accumulation (%) = RI counts of liver homogenate sample (dpm) / RI counts of injected total carriers labeled with [^{3}H]-CHE x100

Mitochondrial targeting activity (/mg mitochondria) = RI counts of mitochondria-enriched fraction (dpm/mg mitochondria) / RI counts of injected total carriers labeled with [^{3}H]-CHE

2.10. Evaluation of hepatoprotective effect from I/R injury after systemic injection of CoQ_{10}-MITO-Porter.

To evaluate anti-oxidant effects, we used hepatic I/R injury induced mice that overexpress mitochondrial ROS in the liver. In this experiment, it was assumed that the ROS damaged hepatocytes and the intracellular ALT would leak out of the cell, resulting in an increase in serum ALT levels. Samples containing CoQ_{10} were administered to mice at a dose of 2.0 mg/kg CoQ_{10} in a total volume of 10 mL/kg. Mice were treated with naked CoQ_{10} and MitoQ in 100% (v/v) EtOH *via* an intraperitoneal injection and with other samples in PBS (-) *via* an intravenous injection. At 18-hr after the injection of the samples, hepatic I/R injury was induced, according to a previous report [22]. General anesthesia was induced by inhalation of the anesthetic, isoflurane. After laparotomy, all vessels (hepatic artery, portal vein, and bile duct) to the left and median liver lobes were clamped. After 60 min of ischemia, these vessels were unclamped and the circulation was restored for the specified reperfusion time period before killing the animal. At 3-hr after the reperfusion of the liver, blood was collected, followed by incubation at centrifugation at room temperature for 1 hr. To obtain serum, blood samples were centrifuged at 800*g* at 4°C for 5 min. Serum ALT- and aspartate aminotransferase (AST)-levels were then determined using a commercially available kit (Wako Pure Chemical Industries, Ltd. Osaka, Japan).

2.11. Statistical Analysis

Data are expressed as the mean ± S.D. for the indicated number of experiments. Statistical significances between two groups were examined by the unpaired student's *t*-test (Figure 2C and Figure 6B). For multiple comparisons, one way ANOVA was performed (Figures 4A, 4B, Figure 5 and Figure 6C). Levels of $P < 0.05$ were considered to be significant.

3. Results

3.1. Distribution of the MITO-Porter in liver tissue and mitochondrial accumulation

We first investigated the distribution of the MITO-Porter in the liver after systemic injection of the carriers. We prepared the MITO-Porter with highly mitochondrial fusogenic envelopes [5, 9, 11, 21],

where, of the total lipids, 10 mol% R8 was modified on the carrier surface, by the hydration method. We also prepared PEG-LP without R8 as a control carrier. The physiochemical properties of these carriers are summarized in Table S1. For histological observations, carriers labeled with DiI (red color) were intravenously administered to mice *via* the tail vein at a dose of 2.75 μmol lipids/kg. At 1-hr after the injection, the liver tissue was analyzed by CLSM after staining the nuclei with Hoechst 33342 (blue color) and blood vessels FITC-isolection B4 (green color) (Figure 2A). As a result, we confirmed that numerous strong red signals corresponding to the MITO-Porter had accumulated in the liver cells ((b) in Figure 2A), while only weak signals derived from PEG-LP were observed ((c) in Figure 2A).

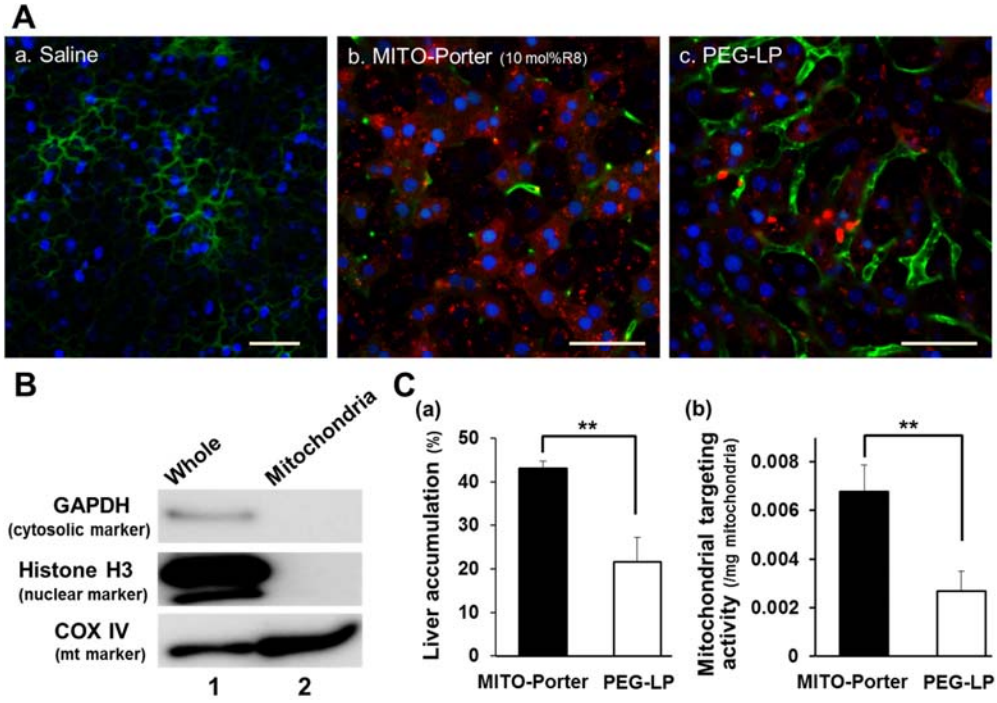

Fig. 2. Distribution of the MITO-Porter in liver tissue and quantification of mitochondrial accumulation. (A) Histological observation of liver. Mice were treated with DiI labeled carriers (red color) administered by intravenous injection (2.75 μmol lipids/kg). At 1-hr after injection, the liver tissue was analyzed by CLSM; saline administered liver (a), MITO-Porter (10 mol% of R8) administered liver (b) and PEG-LP administered liver (c). Nuclei were stained blue with Hoechst 33342 and blood vessels were stained green with FITC-isolection B4. Scale bars, 50 μm. (B) Western blot analysis of mitochondria-enriched fraction obtained from the liver. Each sample (5 μg of protein) was subjected to Western blotting. Primary antibodies from the mouse against COX IV, Histone H3 and GAPDH, as mitochondrial, nuclear and cytosolic fraction markers, were used. Whole and Mitochondria indicate the whole fraction containing homogenate of livers and the mitochondria-enriched fraction, respectively. (C) Quantification of carrier accumulation in liver mitochondria by RI. MITO-Porter (10 mol% of R8) and PEG-LP labeled with [^{3}H]-CHE were systemically injected into the tail vein of mice (2.75 μmol lipids/kg). The values for liver accumulation (a) and mitochondrial targeting activity (/mg mitochondria) (b) were calculated from the count of [^{3}H] in liver and mitochondrial lysate 1 hr after injection as described in Materials and methods. Bars indicate means ± S.D. (n=3-5). **Significant differences ($p<0.01$) between MITO-Porter and PEG-LP were calculated by an unpaired Student's t-test.

We then quantified the accumulation of the carrier in liver mitochondria after systemic injection. To verify the mitochondrial delivery in the liver, the purity of the isolated mitochondria must be verified. In this experiment, the livers were harvested following systemic injection and homogenized, and the mitochondria-enriched fraction was then isolated from the homogenate by differential centrifugation, as

described in a previous report [11, 23]. Samples of the homogenate and mitochondria-enriched fraction were subjected to Western blotting using primary antibodies against COX IV, Histone H3 and GAPDH, as mitochondrial, nuclear and cytosolic fraction markers (Figure 2B). The data showed that only a band corresponding to COX IV was detected in the mitochondria-enriched fraction (lane 2 in Figure 2B), indicating that the mitochondria were exclusively isolated from the liver.

In this experiment, we prepared a MITO-Porter and PEG-LP with similar lipid compositions described above, as shown in Table S1, and the carriers labeled with [^{3}H]-CHE were then administered to mice *via* tail vein injection (2.75 μmol lipids/kg). At 1-hr after the administration, each animal was sacrificed, and the values of liver accumulation ((a) in Figure 2C) and mitochondrial targeting activity (/dose) ((b) in Figure 2C) were estimated from the [^{3}H] content in the liver and mitochondrial lysate. As shown in Figure 2C (a), the MITO-Porter accumulated in the liver much more efficiently than PEG-LP. This result is in agreement with the histological observations shown in Figure 2A. Moreover, we confirmed that the use of the MITO-Porter resulted in a significant increase in mitochondrial targeting activity compared with that for PEG-LP ((b) in Figure 2C)). These results indicate that the MITO-Porter that was validated for mitochondrial delivery in cultured cells was also able to reach the liver *via* systemic injection, followed by mitochondrial targeting in the liver.

3.2. Construction of CoQ_{10}-MITO-Porter and visualization of the carriers in liver tissue

To reach hepatocytes after systemic administration of the CoQ_{10}-MITO-Porter, the carrier is required to pass through small pores in endothelial cells (fenestra) as shown in Figure 1. It is known that the size of the fenestra of mice are around 140 nm [24], thus controlling the size of carrier would play an important role in the delivery of the carrier to hepatocytes. In this experiment, we prepared CoQ_{10}-MITO-Porters with different diameters, and investigated the effect of carrier size on liver accumulation. Figure 3A shows a schematic diagram of the preparation of the CoQ_{10}-MITO-Porter by the ethanol dilution method. The construction of the carriers requires the following 4 steps: (1) dilution of the EtOH solution dissolving the lipids and CoQ_{10} with a buffer to a concentration of 90% EtOH for small sized carriers or 50% EtOH for large sized carriers, (2) finally to a concentration of ~5% EtOH, (3) EtOH

Table 1. Physicochemical properties of small and large sized CoQ_{10}-MITO-Porter.

	Diameters (nm)	PDI	ζ-potentials (mV)
Small sized CoQ_{10}-MITO-Porter	84±7	0.26±0.05	29±1
Large sized CoQ_{10}-MITO-Porter	316±44	0.24±0.08	31±6

These carriers composed of DOPE/SM/STR-R8/DMG-PEG2000/CoQ_{10} [9/2/1.1/0.33/1.8, molar ratio]. The carriers labeled with 0.5 mol% DiI were prepared. Data are means ± S.D. (n=3).

removal by ultrafiltration (<0.1%) and (4) R8 modification. The physicochemical properties of the carriers are summarized in Table 1. As a result, we succeeded in preparing a CoQ_{10}-MITO-Porter with a diameter of less than 100 nm (small sized CoQ_{10}-MITO-Porter) and a large sized CoQ_{10}-MITO-Porter with a diameter of about 300 nm. Both carriers had a positive charge, indicating that the R8 (cationic peptide) can be modified on the surface of the carriers (10 mol% of R8 per total lipids).

We then investigated the accumulation of the carriers in the liver after systemic administration using fluorescent imaging. DiI labeled CoQ_{10}-MITO-Porters (10 mol% of R8) (red color) were administrated to mice *via* tail vein injection (3.5 μmol lipids/kg). At 1-hr after the injection, liver tissue was analyzed by CLSM after staining the nuclei (blue color) and blood vessels (green color) as described above (Figure 3B). As a result, we observed that numerous strong red signals had accumulated in the liver cells in the case of small sized CoQ_{10}-MITO-Porter ((b) in Figure 3B). On the other hand, only very weak signals in the liver were observed in the case of the large sized CoQ_{10}-MITO-Porter ((c) in Figure 3B), indicating that an optimal size of the CoQ_{10}-MITO-Porter is needed to pass through fenestra to reach hepatocytes. Thus, we concluded that the size control of the CoQ_{10}-MITO-Porter is an important factor in the accumulation of the carriers in the livers *via* systemic injection.

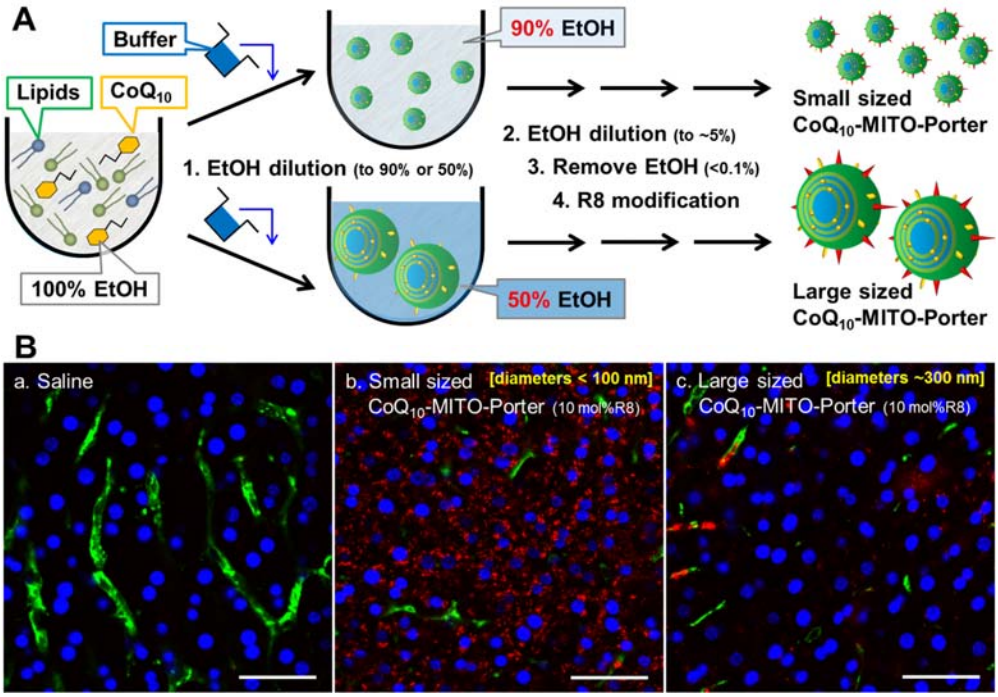

Fig. 3. Investigation of the size effect of the CoQ_{10}-MITO-Porter on the distribution of the carrier in liver tissue. (**A**) Schematic diagram showing the preparation of the CoQ_{10}-MITO-Porter by the ethanol dilution method and the size control. The construction of the CoQ_{10}-MITO-Porter requires the following 4 steps: (1) dilution of the EtOH solution containing the dissolved the lipids and CoQ_{10} with a buffer to a concentration of 90% EtOH for small sized carriers or 50% EtOH for large sized carriers, (2) finally to a concentration of ~5% EtOH, (3) EtOH removal by ultrafiltration (<0.1%) and (4) R8 modification. (**B**) Histological observation of liver. Mice were treated with DiI labeled CoQ_{10}-MITO-Porters (10 mol% of R8) (red color) administered by intravenous injection (3.5 μmol lipids/kg). At 1-hr injection, the liver tissue was analyzed by CLSM; saline administered liver (a), small sized CoQ_{10}-MITO-Porter administered liver (b) and large sized CoQ_{10}-MITO-Porter administered liver (c). Nuclei were stained blue with Hoechst 33342 and blood vessels were stained green with FITC-isolection B4. Scale bars, 50 μm.

3.3. Optimization of mitochondrial binding and fusion activities of the CoQ10-MITO-Porter and the fluorescent imaging of the carriers in liver tissue

In an I/R injury induced mice liver, ROS are mainly produced in the mitochondrial respiratory chain which is localized on the mitochondrial inner membrane. Thus, to be effective, CoQ_{10} must be delivered to the mitochondrial inner membrane. We subsequently investigated the mitochondrial binding and membrane fusion activities of the CoQ_{10}-MITO-Porter that contained PEG and CoQ_{10} with various ratios of R8. For a mitochondrial binding assay and a mitochondrial fusogenic activity assay, carriers containing NBD-DOPE and dual-labeled carriers containing both NBD-DOPE and rhodamine-DOPE were prepared, respectively. The physicochemical properties of the carriers are summarized in Table 2. The particle diameters were less than 100

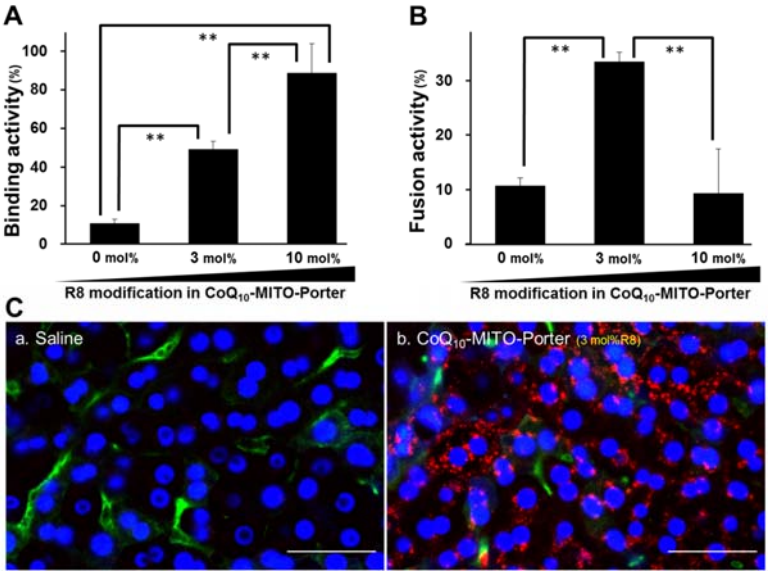

Fig. 4. The mitochondrial binding and fusogenic activities of the CoQ10-MITO-Porter and the histological observation in the liver. (A) and (B) indicate mitochondrial binding activities and mitochondrial fusogenic activities of CoQ10-MITO-Porter modified with different amounts of R8, respectively. Data are means ± S.D. (n=3). **Significant differences ($p<0.01$) were calculated by one-way ANOVA, followed by Student-Newman-Keuls (SNK) test. (C) Histological observation of CoQ10-MITO-Porter (3 mol% of R8) in the liver. Liver tissues after systemic injection of the carrier (7 μmol lipids/kg) labeled with DiI (pseudo red color) were observed CLSM, after staining nuclei with Hoechst 33342 (blue) and blood vessels with fluorescein-isolectin B4 (green). Liver tissues derived from the mice (a) saline administration and (b) treated with the CoQ10-MITO-Porter. Scale bars, 50 μm.

Table 2. Characteristics of carriers prepared for binding and fusion assays.

CoQ_{10}-MITO-Porter-type	Compositions (molar ratio)	R8-modification (mol% of lipids)	Size (nm)	PDI	ζ-potential (mV)
CoQ_{10}-MITO-Porters for binding assay	DOPE/SM/DMG-PEG2000/CoQ_{10}/NBD-DOPE/*STR-R8* (9/2/0.33/1.8/0.13/*X*)	0	72±2	0.28±0.04	-7.5±1
		3	71±1	0.27±0.04	18±2
		10	70±1	0.23±0.02	27±1
CoQ_{10}-MITO-Porters for fusogenic assay	DOPE/SM/DMG-PEG2000/CoQ_{10}/NBD-DOPE/rhodamine-DOPE/*STR-R8* (9/2/0.33/1.8/0.13/0.066/*X*)	0	75±6	0.26±0.04	-11±2
		3	74±4	0.25±0.02	19±3
		10	73±7	0.23±0.03	25±4
CoQ_{10}-MITO-Porters for histological observation	DOPE/SM/DMG-PEG2000/CoQ_{10}/DiI/*STR-R8* (9/2/0.33/1.8/0.066/*X*)	3	88±5	0.29±0.05	16±5

Data are means ± S.D. (n=3).

nm and the ζ-potentials increased with increasing ratios of R8-modification. As shown in Figure 4A, the mitochondrial binding activity was increased, when the R8 modification was increased in the CoQ_{10}-MITO-Porter. It was also that confirmed that the membrane fusion of CoQ_{10}-MITO-Porter modified with 3 mol% of R8 had the highest activity, among the particles tested (Figure 4B).

We then obtained fluorescent images of the liver tissues after the systemic injection of the CoQ_{10}-MITO-Porter modified with 3 mol% of R8 labeled with DiI (red) using CLSM, to verify whether the carriers were delivered to liver mitochondria the same as the CoQ_{10}-MITO-Porter modified with 10 mol% of R8, as shown in Figure 3B. The physicochemical properties of the carriers were analyzed, and the results were confirmed that a positively charged particle with a diameter of around 90 nm was prepared (Table 2). The encapsulation efficiency of CoQ_{10} into the MITO-Porter was high (86.3±3%, n=3). As shown in Figure 4C, the fluorescent labeled carriers had effectively accumulated in the liver, as evidenced by the red signals.

We also quantified the carrier accumulation in liver mitochondria after systemic injection by a similar procedure using RI labeled carriers as described above. As shown in Figure S1, the CoQ_{10}-MITO-Porter modified with 3 mol% of R8 accumulated in the liver and the mitochondria efficiently as well as the MITO-Porter without CoQ_{10}. Moreover, we investigated the stability of CoQ_{10}-MITO-Porter in serum *via in vitro* experiments, where the carriers were incubated with/without serum at 37ºC, followed by measuring the diameters of the particles. The findings indicated that the diameters of the carriers were comparable in presence/absence of serum (Figure S3), suggesting that the CoQ_{10}-MITO-Porter did not undergo aggregation in the serum within the 1 hr time period needed for it to accumulate in the liver. These results indicate that the CoQ_{10}-MITO-Porter that was optimized for mitochondria fusogenic activity are able to reach the liver mitochondria *via* systemic injection. We used a CoQ_{10}-MITO-Porter modified with 3 mol% R8 as the CoQ_{10}-MITO-Porter in the following experiment.

3.4. Evaluation of protection from hepatic I/R injury by mitochondrial delivery of CoQ_{10} using MITO-Porter

To evaluate anti-oxidant effects, we used hepatic I/R injury model mice that overexpress mitochondrial ROS, where serum ALT levels would be expected to be increased. We confirmed that the magnitude of the serum ALT-levels of the hepatic I/R injury model mice were thousands of the value as shown in Figure 5, while the value for normal mice was only several dozen (29±15 IU/L, n=3). This result is in general agreement with results from a previous report stating that serum ALT-levels of hepatic I/R injury model mice to normal mice showed an extremely high value [15, 22], indicating that the I/R injury is actually caused in the liver of our model mouse.

We expected that the mitochondrial delivery of CoQ_{10} (an antioxidant) to the I/R injury induced mice liver would protect the liver from mitochondria-derived ROS, resulting in a decrease in ALT levels. In this experiment, we administered samples containing CoQ_{10} to mice *via* intravenous injection (vehicle, CoQ_{10}-MITO-Porter) and intraperitoneal injection (naked CoQ_{10}, MitoQ), and induced hepatic I/R injury, followed by measuring serum ALT levels. The accumulation of these carriers in the normal liver might be different from that in a liver that had been damaged by an I/R injury. In our protocol, we administered the carriers containing CoQ_{10} before the hepatic I/R injury, based on a previous study [15]. Thus, we were able to evaluate the anti-oxidant effect in terms of the biodistribution of the carrier in normal mice.

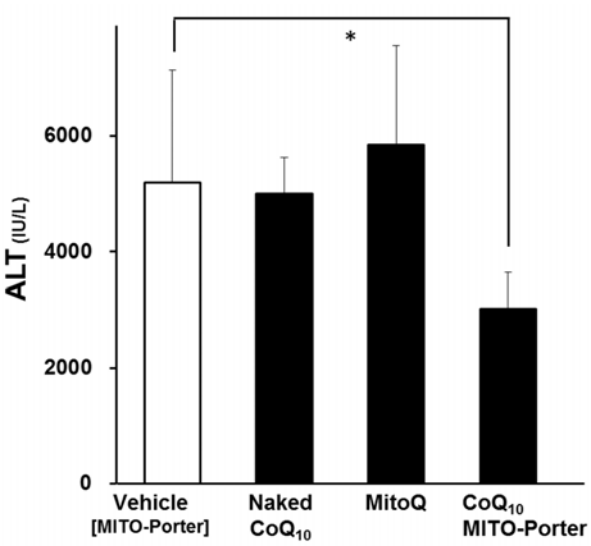

Fig. 5. Evaluation of hepatoprotective effect from I/R injury. Samples containing CoQ_{10} were administered into mice *via* intravenous injection (vehicle, CoQ_{10}-MITO-Porter) and intraperitoneal injection (naked CoQ_{10}, MitoQ). MITO-Porter (DOPE/SM/DMG-PEG2000/STR-R8=9/2/0.33/1.1, molar ratio) was used as a vehicle. Serum ALT activities were measured after the hepatic I/R injury. Data are represented as the mean ± S.D. (n = 4). *Significant difference between vehicle and others ($p < 0.05$ by one-way ANOVA, followed by Bonferroni test).

Table 3. Characteristics of the carriers used to evaluate the hepatoprotective effect from an I/R injury.

	Lipid compositions [molar ratio]	Diameters (nm)	PDI	ζ-potentials (mV)
Vehicle [MITO-Porter]	DOPE/SM/STR-R8/DMG-PEG2000 [9/2/1.1/0.33]	78±4	0.31±0.05	28±2
CoQ_{10}-MITO-Porter	DOPE/SM/STR-R8/DMG-PEG2000/CoQ_{10} [9/2/0.33/0.33/1.8]	82±1	0.21±0.03	23±2
Vehicle [EPC-LP]	EPE/SM/STR-R8/DMG-PEG2000 [9/2/1.1/0.33]	51±6	0.39±0.05	22±2
CoQ_{10}-EPC-LP	EPE/SM/DMG-PEG2000/CoQ_{10} [9/2/0.33/1.8]	44±1	0.27±0.01	-2.4±1
CoQ_{10}-R8-EPC-LP	EPC/SM/STR-R8/DMG-PEG2000/CoQ_{10} [9/2/1.1/0.33/1.8]	45±1	0.30±0.01	23±4

Data are means ± S.D. (n=3-5).

The MITO-Porter (DOPE/SM/DMG-PEG2000/STR-R8=9/2/0.33/1.1, molar ratio) was used as a vehicle. The physicochemical properties of the materials used in this evaluation are summarized in Table 3. We also used MitoQ as a positive control of a mitochondrial targeting antioxidant. As shown in Figure 5, the CoQ_{10}-MITO-Porter resulted in a significant decrease in serum ALT levels compared with

naked CoQ_{10} and MitoQ. These results suggest that the systemic injection of the CoQ_{10}-MITO-Porter permits CoQ_{10} to be delivered to liver mitochondria, thus decreasing mitochondrial ROS levels.

4. Discussion

We confirmed the utility of a mitochondrial therapeutic strategy that involves targeting *in vivo* mitochondria using a MITO-Porter, which delivered therapeutic cargoes to mitochondria and showed a mitochondrial therapeutic effect as well as in an *in vitro* experiment [12, 13]. In the present study, the MITO-Porter was designed to deliver therapeutic cargoes to liver mitochondria of mice *via* systemic injection for prevention of hepatic I/R injury. Thus, we first investigated the distribution of the MITO-Porter in the liver after systemic injection of the carriers. Fortunately, the systemic injection of a MITO-Porter, in which the carrier surface was modified with R8, proved to be effective for targeting liver tissue, as shown in Figures 2A and 2C(a). We previously reported that intravenously injected R8-modified carriers effectively accumulated in the liver, resulting in a high transgene expression [25].

Previous biodistribution studies showed that the R8-modified carriers rapidly accumulated in the liver within 10 min and that the accumulation in other tissues including kidney, lung and spleen were significantly lower compared to the liver [26, 27]. We confirmed the same tendency that the liver accumulation of the CoQ_{10}-MITO-Porter (10 mol% of R8) was higher than in other tissues (Figure S4). Although the mechanism responsible for the liver accumulation of R8-modified carriers is unknown, it is possible that R8 might function as a specific ligand for hepatocytes and that carriers with a cationic charge could be recognized by macrophages of the liver. In future studies, we plan to investigate the distribution of MITO-Porter between hepatocytes and hepatic macrophages in mice livers after the systemic injection.

Moreover, we confirmed that the MITO-Porter localized in mitochondria in the liver, as shown in Figure 2C(b). A previous investigation using isolated rat liver mitochondria showed that the modification of the carrier-surface with R8 significantly enhanced binding to mitochondria [5]. A similar result was observed in the case of mitochondria isolated from the livers of mice (data not shown). Thus, we concluded that the R8 contained in the MITO-Porter was an important factor in the successful accumulation of the carriers in the liver, when administered by systemic injection and that mitochondrial targeting had been achieved.

We also investigated the effect of the size of the carrier on the liver accumulation *via* the systemic injection, because the carrier is required to pass through fenestra to reach the hepatocyte as

shown in Figure 1. It is known that fenestra are small pores in the vascular endothelial cells of the sinusoid, and the size of fenestra vary with species [24]. As shown in Figure 3B (b), we observed that numerous carriers had accumulated in the liver cells after systemic injection of a small sized CoQ_{10}-MITO-Porter with a diameter less than 100 nm. It is presumed that the small sized carriers would be able to easily pass through the fenestra of mice with a diameter around 140 nm [24], while the large sized carriers with a diameter more than 300 nm would pass only with difficulty (Figure 3B (c)). On the other hand, the MITO-Porter with a diameter of around 200 nm would be slightly larger than the fenestra size of mice and probably would be able to pass the fenestra (Figure 2A(b) and 2C(a)), because the fenestra size for a mouse is around 140 nm and has wide size distribution. In the case of humans, the fenestra size is around 100 nm and the size distribution is quite narrow [28]. Thus, the size control of the carrier would play a more important role, in carriers accumulating in the human liver when administered *via* systemic injection.

While, the MITO-Porter could be recognized by the reticuloendothelial system, which includes Kupffer cells of the liver and the splenic macrophages. In such a case, the MITO-Porter that accumulated in the liver would be distributed in both hepatocytes and Kupffer cells. On the other hand, biodistribution studies (Figure S4) indicated that the MITO-Porter effectively accumulated in the liver escaping from splenic macrophages. This result is agreement with findings of a previous report in which R8-modified carriers with diameters less than 200 nm accumulated in the liver more efficiently than in the spleen [26, 27]. The cause of this phenomenon may be explained by the previous reports showing that the liposome size affects the biodistribution after the systemic injection of the carriers [29, 30]. In that study, liposomes containing ganglioside GM_1 with a diameter in excess of 300 nm were trapped by splenic macrophages and disappeared in the blood circulation, while the optimal size range of liposomes for a high blood concentration were from 70 to 200 nm [30]. Collectively, it was presumed that the MITO-Porter (diameter = around 200 nm) and the small sized CoQ_{10}-MITO-Porter (diameter < 100 nm) avoided uptake by the spleen, and the carriers modified with R8 then accumulated in the liver. Since ROS are produced in various cell types of liver cells (e.g., hepatocytes, endhothelial, and Kupffer cells) during hepatic I/R injury, the hepatic antioxidant effect resulting from the systemic injection of the CoQ_{10}-MITO-Porter was also contributed by the uptake of CoQ_{10} by Kupffer cells.

CoQ_{10} has a benzoquinone ring linked to 10 isoprene units, is a well-known antioxidant which has properties that are potentially beneficial for preventing cellular damage during an I/R injury [31, 32]. However CoQ_{10} has highly hydrophobic characteristics and a negative charge, which limits its accessibility in naked form to the intracellular mitochondria, which possess a highly negative charge. To date, a number of studies focusing on pharmaceutical formulations of CoQ_{10} have been reported in

attempts to improve the low bioavailability of the largely insoluble CoQ_{10} [32, 33]. In the present study, we designed a CoQ_{10}-MITO-Porter, in which CoQ_{10} was contained in a mitochondria–fusogenic lipid composition and attempted to deliver it to mitochondria. In a previous study, we described the preparation of a MITO-Porter by the hydration method, a relatively easy and simple method [11]. We first attempted to prepare a CoQ_{10}-MITO-Porter using the same procedure, which includes the formation of a lipid film for the MITO-Porter with CoQ_{10} on the bottom of a glass tube, hydration of the lipid film with a buffer and sonication to produce vesicles. However, the methods were not optimal in this case, because it was not possible to remove the CoQ_{10} from the glass tube. Therefore, we investigated the preparation of a CoQ_{10}-MITO-Porter by the ethanol dilution method and reverse phase evaporation method, which do not involve the process of the lipid formation. Both preparation methods permitted the construction of a CoQ_{10}-MITO-Porter. In this experiment, we adopted the ethanol dilution method, because, using this method, it is relatively easy to control the size of the CoQ_{10} containing carriers by just varying a concentration of EtOH in the presence of PEG-lipids.

A FRET analysis using isolated mouse mitochondria showed that the mitochondrial membrane fusion of CoQ_{10}-MITO-Porter modified with 3 mol% of R8 was significantly higher than that prepared with 10 mol% of R8 (Figure 4B). While, a conventional MITO-Porter without CoQ_{10} and PEG (DOPE/SM/STR-R8 = 9/2/1, molar ratio) showed a high membrane fusion activity with mouse liver mitochondria (76±11%, n=3). Thus, we concluded that the CoQ_{10} and PEG contained in CoQ_{10}-MITO-Porter affected the mitochondrial membrane fusion property of the carrier. On the other hand, the mitochondrial binding activity was increased, when the R8 modification was increased in the CoQ_{10}-MITO-Porter (Figure 4A). As shown in Table 2, the ζ-potentials of the CoQ_{10}-MITO-Porter were increased with increasing R8-modification. This suggests that R8 modification results in a positive charge on the carrier surface, which largely contributes to mitochondrial binding with the carriers *via* electrostatic interactions.

To evaluate the anti-oxidant effects of the CoQ_{10}-MITO-Porter, we used MitoQ (Figure S2A) as a positive control for a mitochondrial targeting antioxidant. To date, the utilities of a therapeutic strategy using MitoQ have been demonstrated in *in vivo* experiments using various disease model animals [15, 34-36]. Moreover, MitoQ has been investigated in clinical trials [20, 37, 38] and is expected to be promising candidate for a mitochondrial medicine. MitoQ was also investigated for protection of the liver and heart from I/R injury in *in vivo* experiments using I/R injury induced mice and rats [15, 39, 40]. We synthesized MitoQ essentially as described in a previous report [20], and confirmed that the MitoQ was actually produced as evidenced by MS analyses for the MitoQ (calculated MW583 and observed

MW583.3). Further analyses using ^{1}H NMR spectroscopy and ^{31}P NMR spectroscopy verified the successful synthesis of MitoQ (data not shown).

To validate therapeutic effect of the synthesized MitoQ, we administered MitoQ in an EtOH suspension to mice *via* intraperitoneal injection, and induced a hepatic I/R injury, followed by measuring the serum ALT levels (Figure S2B), using 100% EtOH as a vehicle. A dose of 5.0 mg/kg CoQ_{10} resulted in a therapeutic effect, while the administration of 2.5 mg/kg of CoQ_{10} was comparable with vehicle in serum ALT levels. In a previous report [15], the administration of 1.0 mg/kg CoQ_{10} to mice *via* intraperitoneal injection showed a therapeutic effect. The difference in the applied dose for a therapeutic effect with the present study can be attributed to differences in the experiment conditions used.

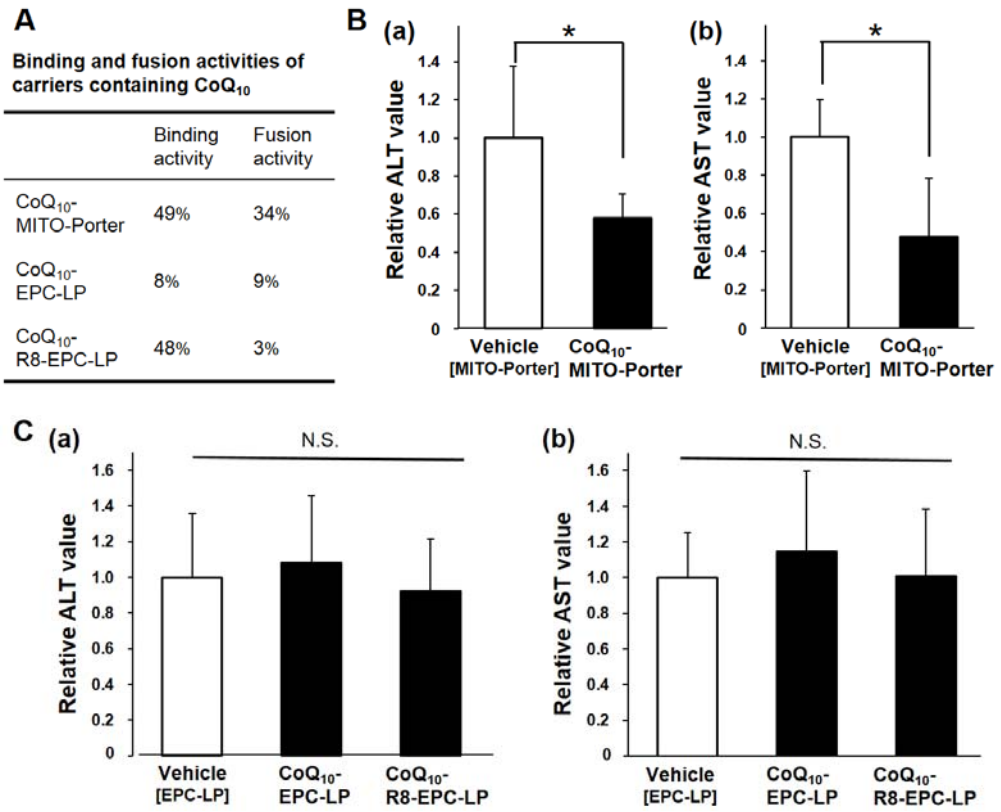

Fig. 6. Investigation for binding and fusion activities of carriers on the hepatoprotective effect from I/R injury. Carriers containing CoQ_{10} with different binding and fusion activities were administered into mice *via* intravenous injection. The binding and fusion activities of carriers are summarized in Figure 6A. The values for CoQ_{10}-MITO-Porter (3 mol% of R8), data shown in Figure 4 were used. MITO-Porter and EPC-LP were used as vehicles (see the Table 3 for the detail). Relative ALT value (a) and AST value (b) were evaluated after the hepatic I/R injury (B, C). Data are represented as the mean ± S.D. (n = 4-6). In Figure 6B, significant differences were determined by unpaired Student' s t-test (*p < 0.05). In Figure 6C, significant differences between vehicle and others were calculated by one-way ANOVA, and no significant difference (N.S.) was found.

As shown in Figure 5, the systemic injection of the CoQ_{10}-MITO-Porter achieved protection from a hepatic I/R injury. We conclude that this therapeutic effect resulted from the delivery of CoQ_{10} to mice liver mitochondria by the MITO-Porter *via* membrane fusion. To validate this issue, we investigated the mitochondrial binding and fusion activities of carriers on protection from hepatic I/R injury. In this experiment, we prepared a CoQ_{10}-EPC-LP with low binding and fusion activities and CoQ_{10}-R8-EPC-LP with high binding and low fusion activities. For the mitochondrial binding assay and

mitochondrial fusogenic activity assay, fluorescent labeled carriers were prepared and the physicochemical properties of the carriers are summarized in Table S2, and the mitochondrial binding and fusion activities are shown in Figure 6A. For the values for the CoQ_{10}-MITO-Porter (3 mol% of R8), the data shown in Figures 4A and 4B were used.

We then administered samples containing CoQ_{10} to mice *via* intravenous injection, and induced hepatic I/R injury, followed by measuring the serum ALT and AST levels. The physicochemical properties used in this evaluation are summarized in Table 3. As shown in Figure 6 B, the CoQ_{10}-MITO-Porter with high binding and fusion activities resulted in a significant decrease in serum ALT and AST levels compared with Vehicle. On the other hand, neither CoQ_{10}-EPC-LP nor CoQ_{10}-R8-EPC-LP had a measurable therapeutic effect (Figure 6 C). CoQ_{10}-R8-EPC-LP, which was modified with R8 on the carrier-surface, would reach liver mitochondria at same level of CoQ_{10}-MITO-Porter, while the mitochondrial membrane fusion activity of the carrier was very low (3%) as shown in Figure 6A. These results suggest that the mitochondrial membrane fusion activity of the CoQ_{10}-MITO-Porter is an important factor in the development of a therapeutic effect for hepatic I/R injury induced mice.

5. Conclusion

We report on the successful delivery of CoQ_{10} to liver mitochondria of mice *via* the systemic injection of a CoQ_{10}-MITO-Porter. We confirmed that controlling the size of the carrier is an important factor and that the use of R8 contributed to liver accumulation and the mitochondrial targeting. We also confirmed that the *in vivo* mitochondrial delivery of CoQ_{10} *via* MITO-Porter prevents the development of hepatic I/R injury. Moreover, the findings show that the mitochondrial membrane fusion activity of the CoQ_{10}-MITO-Porter largely contributed to the therapeutic effect for the hepatic I/R injury. This provides a demonstration that the MITO-Porter represents a potentially useful carrier for use in mitochondrial medicine.

Acknowledgement

This work was supported, in part by, a Grant-in-Aid for Young Scientists (A) [Grant No. 23680053 (to Y.Y.)] from the Ministry of Education, Culture, Sports, Science and Technology, the Japanese Government (MEXT), and A-step feasibility study program in Japan Science and Technology Agency (JST) [Grant No. AS251Z00277Q (to Y.Y.)], Northern Advancement Center for Science & Technology

(Noastec Foundation,. Hokkaido, Japan) [Grant No. T-1-42 (to Y.Y.)], the Mochida Memorial Foundation for Medical and Pharmaceutical Research. We are grateful to Dr. Yusuke Sato (Hokkaido University, Japan) for his helpful comments with the experiment to investigate the stability of carrier in serum. We also thank Dr. Milton Feather for his helpful advice in writing the manuscript.

Tables

Table 1. Physicochemical properties of small and large sized CoQ_{10}-MITO-Porter.

	Diameters (nm)	PDI	ζ-potentials (mV)
Small sized CoQ_{10}-MITO-Porter	84±7	0.26±0.05	29±1
Large sized CoQ_{10}-MITO-Porter	316±44	0.24±0.08	31±6

These carriers composed of DOPE/SM/STR-R8/DMG-PEG2000/CoQ_{10} [9/2/1.1/0.33/1.8, molar ratio]. The carriers labeled with 0.5 mol% DiI were prepared. Data are means ± S.D. (n=3).

Table 2. Characteristics of carriers prepared for binding and fusion assays.

CoQ_{10}-MITO-Porter-type	Compositions (molar ratio)	R8-modification (mol% of lipids)	Size (nm)	PDI	ζ-potential (mV)
CoQ_{10}-MITO-Porters for binding assay	DOPE/SM/DMG-PEG2000/CoQ_{10}/NBD-DOPE/*STR-R8* (9/2/0.33/1.8/0.13/*X*)	0	72±2	0.28±0.04	-7.5±1
		3	71±1	0.27±0.04	18±2
		10	70±1	0.23±0.02	27±1
CoQ_{10}-MITO-Porters for fusogenic assay	DOPE/SM/DMG-PEG2000/CoQ_{10}/NBD-DOPE/rhodamine-DOPE/*STR-R8* (9/2/0.33/1.8/0.13/0.066/*X*)	0	75±6	0.26±0.04	-11±2
		3	74±4	0.25±0.02	19±3
		10	73±7	0.23±0.03	25±4
CoQ_{10}-MITO-Porters for histological observation	DOPE/SM/DMG-PEG2000/CoQ_{10}/DiI/*STR-R8* (9/2/0.33/1.8/0.066/*X*)	3	88±5	0.29±0.05	16±5

Data are means ± S.D. (n=3).

Table 3. Characteristics of the carriers used to evaluate the hepatoprotective effect from an I/R injury.

	Lipid compositions [molar ratio]	Diameters (nm)	PDI	ζ-potentials (mV)
Vehicle [MITO-Porter]	DOPE/SM/STR-R8/DMG-PEG2000 [9/2/1.1/0.33]	78±4	0.31±0.05	28±2
CoQ_{10}-MITO-Porter	DOPE/SM/STR-R8/DMG-PEG2000/CoQ_{10} [9/2/0.33/0.33/1.8]	82±1	0.21±0.03	23±2
Vehicle [EPC-LP]	EPE/SM/STR-R8/DMG-PEG2000 [9/2/1.1/0.33]	51±6	0.39±0.05	22±2
CoQ_{10}-EPC-LP	EPE/SM/DMG-PEG2000/CoQ_{10} [9/2/0.33/1.8]	44±1	0.27±0.01	-2.4±1
CoQ_{10}-R8-EPC-LP	EPC/SM/STR-R8/DMG-PEG2000/CoQ_{10} [9/2/1.1/0.33/1.8]	45±1	0.30±0.01	23±4

Data are means ± S.D. (n=3-5).

Figure legends

Figure 1. Schematic image of prevention of the hepatic I/R injury by mitochondrial delivery of CoQ_{10} using MITO-Porter system. CoQ_{10}, coenzyme Q_{10}; I/R, ischemia/reperfusion; ROS, reactive oxygen species.

Figure 2. Distribution of the MITO-Porter in liver tissue and quantification of mitochondrial accumulation. (**A**) Histological observation of liver. Mice were treated with DiI labeled carriers (red color) administered by intravenous injection (2.75 μmol lipids/kg). At 1-hr after injection, the liver tissue was analyzed by CLSM; saline administered liver (a), MITO-Porter (10 mol% of R8) administered liver (b) and PEG-LP administered liver (c). Nuclei were stained blue with Hoechst 33342 and blood vessels were stained green with FITC-isolection B4. Scale bars, 50 μm. (**B**) Western blot analysis of mitochondria-enriched fraction obtained from the liver. Each sample (5 μg of protein) was subjected to Western blotting. Primary antibodies from the mouse against COX IV, Histone H3 and GAPDH, as mitochondrial, nuclear and cytosolic fraction markers, were used. Whole and Mitochondria indicate the whole fraction containing homogenate of livers and the mitochondria-enriched fraction, respectively. (**C**) Quantification of carrier accumulation in liver mitochondria by RI. MITO-Porter (10 mol% of R8) and PEG-LP labeled with [^{3}H]-CHE were systemically injected into the tail vein of mice (2.75 μmol lipids/kg). The values for liver accumulation (a) and mitochondrial targeting activity (/mg mitochondria) (b) were calculated from the count of [^{3}H] in liver and mitochondrial lysate 1 hr after injection as described in Materials and methods. Bars indicate means ± S.D. (n=3-5). **Significant differences ($p<0.01$) between MITO-Porter and PEG-LP were calculated by an unpaired Student's t-test.

Figure 3. Investigation of the size effect of the CoQ_{10}-MITO-Porter on the distribution of the carrier in liver tissue. (**A**) Schematic diagram showing the preparation of the CoQ_{10}-MITO-Porter by the ethanol dilution method and the size control. The construction of the CoQ_{10}-MITO-Porter requires the following 4 steps: (1) dilution of the EtOH solution containing the dissolved lipids and CoQ_{10} with a buffer to a concentration of 90% EtOH for small sized carriers or 50% EtOH for large sized carriers, (2) finally to a concentration of ~5% EtOH, (3) EtOH removal by ultrafiltration (<0.1%) and (4) R8 modification. (**B**) Histological observation of liver. Mice were treated with DiI labeled CoQ_{10}-MITO-Porters (10 mol% of R8) (red color) administered by intravenous injection (3.5 μmol lipids/kg). At 1-hr injection, the liver tissue was analyzed by CLSM; saline administered liver (a), small sized CoQ_{10}-MITO-Porter

administered liver (b) and large sized CoQ_{10}-MITO-Porter administered liver (c). Nuclei were stained blue with Hoechst 33342 and blood vessels were stained green with FITC-isolection B4. Scale bars, 50 μm.

Figure 4. The mitochondrial binding and fusogenic activities of the CoQ_{10}-MITO-Porter and the histological observation in the liver. (**A**) and (**B**) indicate mitochondrial binding activities and mitochondrial fusogenic activities of CoQ_{10}-MITO-Porter modified with different amounts of R8, respectively. Data are means ± S.D. (n=3). **Significant differences ($p<0.01$) were calculated by one-way ANOVA, followed by Student-Newman-Keuls (SNK) test. (**C**) Histological observation of CoQ_{10}-MITO-Porter (3 mol% of R8) in the liver. Liver tissues after systemic injection of the carrier (7 μmol lipids/kg) labeled with DiI (pseudo red color) were observed CLSM, after staining nuclei with Hoechst 33342 (blue) and blood vessels with fluorescein-isolectin B4 (green). Liver tissues derived from the mice (a) saline administration and (b) treated with the CoQ_{10}-MITO-Porter. Scale bars, 50 μm.

Figure 5. Evaluation of hepatoprotective effect from I/R injury. Samples containing CoQ_{10} were administered into mice via intravenous injection (vehicle, CoQ_{10}-MITO-Porter) and intraperitoneal injection (naked CoQ_{10}, MitoQ). MITO-Porter (DOPE/SM/DMG-PEG2000/STR-R8=9/2/0.33/1.1, molar ratio) was used as a vehicle. Serum ALT activities were measured after the hepatic I/R injury. Data are represented as the mean ± S.D. (n = 4). *Significant difference between vehicle and others ($p < 0.05$ by one-way ANOVA, followed by Bonferroni test).

Figure 6. Investigation for binding and fusion activities of carriers on the hepatoprotective effect from I/R injury. Carriers containing CoQ_{10} with different binding and fusion activities were administered into mice *via* intravenous injection. The binding and fusion activities of carriers are summarized in Figure 6A. For the values of CoQ_{10}-MITO-Porter (3 mol% of R8), data shown in Figure 4 were used. MITO-Porter and EPC-LP were used as vehicles (see the Table 3 for the detail). Relative ALT value (a) and AST value (b) were evaluated after the hepatic I/R injury (B, C). Data are represented as the mean ± S.D. (n = 4-6). In Figure 6B, significant differences were determined by unpaired Student' s t-test (*$p < 0.05$). In Figure 6C, significant differences between vehicle and others were calculated by one-way ANOVA, and no significant difference (N.S.) was found.

References.

[1] D.C. Chan, Mitochondria: dynamic organelles in disease, aging, and development, Cell, 125 (2006) 1241-1252.
[2] I.J. Holt, A.E. Harding, J.A. Morgan-Hughes, Deletions of muscle mitochondrial DNA in patients with mitochondrial myopathies, Nature, 331 (1988) 717-719.
[3] A.H. Schapira, Mitochondrial diseases, Lancet, 379 (2012) 1825-1834.
[4] E. Zhang, C. Zhang, Y. Su, T. Cheng, C. Shi, Newly developed strategies for multifunctional mitochondria-targeted agents in cancer therapy, Drug Discov Today, 16 (2011) 140-146.
[5] Y. Yamada, H. Harashima, Mitochondrial drug delivery systems for macromolecule and their therapeutic application to mitochondrial diseases, Adv Drug Deliv Rev, 60 (2008) 1439-1462.
[6] V. Weissig, From serendipity to mitochondria-targeted nanocarriers, Pharm Res, 28 (2011) 2657-2668.
[7] K. Kajimoto, Y. Sato, T. Nakamura, Y. Yamada, H. Harashima, Multifunctional envelope-type nano device for controlled intracellular trafficking and selective targeting in vivo, J Control Release, 190C (2014) 593-606.
[8] S. Biswas, V.P. Torchilin, Nanopreparations for organelle-specific delivery in cancer, Adv Drug Deliv Rev, 66 (2014) 26-41.
[9] Y. Yamada, H. Harashima, A method for screening mitochondrial fusogenic envelopes for use in mitochondrial drug delivery, Methods Mol Biol, 1141 (2014) 57-66.
[10] T. Endo, Y. Nakayama, M. Nakai, Avidin fusion protein as a tool to generate a stable translocation intermediate spanning the mitochondrial membranes, J Biochem (Tokyo), 118 (1995) 753-759.
[11] Y. Yamada, H. Akita, H. Kamiya, K. Kogure, T. Yamamoto, Y. Shinohara, K. Yamashita, H. Kobayashi, H. Kikuchi, H. Harashima, MITO-Porter: A liposome-based carrier system for delivery of macromolecules into mitochondria via membrane fusion, Biochim Biophys Acta, 1778 (2008) 423-432.
[12] R. Furukawa, Y. Yamada, M. Takenaga, R. Igarashi, H. Harashima, Octaarginine-modified liposomes enhance the anti-oxidant effect of Lecithinized superoxide dismutase by increasing its cellular uptake, Biochem Biophys Res Commun, 404 (2011) 796-801.
[13] Y. Yamada, K. Nakamura, R. Furukawa, E. Kawamura, T. Moriwaki, K. Matsumoto, K. Okuda, M. Shindo, H. Harashima, Mitochondrial delivery of bongkrekic acid using a MITO-porter prevents the induction of apoptosis in human hela cells, Journal of Pharmaceutical Sciences, 102 (2013) 1008-1015.
[14] H. Jaeschke, J.R. Mitchell, Mitochondria and Xanthine-Oxidase Both Generate Reactive Oxygen Species in Isolated Perfused Rat-Liver after Hypoxic Injury, Biochemical and Biophysical Research Communications, 160 (1989) 140-147.
[15] P. Mukhopadhyay, B. Horvath, Z. Zsengeller, S. Batkai, Z. Cao, M. Kechrid, E. Holovac, K. Erdelyi, G. Tanchian, L. Liaudet, I.E. Stillman, J. Joseph, B. Kalyanaraman, P. Pacher, Mitochondrial reactive oxygen species generation triggers inflammatory response and tissue injury associated with hepatic ischemia-reperfusion: therapeutic potential of mitochondrially targeted antioxidants, Free Radic Biol Med, 53 (2012) 1123-1138.
[16] P. Taupin, A dual activity of ROS and oxidative stress on adult neurogenesis and Alzheimer's disease, Cent Nerv Syst Agents Med Chem, 10 (2010) 16-21.
[17] M. Nishikawa, Reactive oxygen species in tumor metastasis, Cancer Lett, 266 (2008) 53-59.
[18] L. Forsberg, U. de Faire, R. Morgenstern, Oxidative stress, human genetic variation, and disease, Archives of Biochemistry and Biophysics, 389 (2001) 84-93.
[19] S. Futaki, W. Ohashi, T. Suzuki, M. Niwa, S. Tanaka, K. Ueda, H. Harashima, Y. Sugiura, Stearylated arginine-rich peptides: a new class of transfection systems, Bioconjug Chem, 12 (2001) 1005-1011.
[20] G.F. Kelso, C.M. Porteous, C.V. Coulter, G. Hughes, W.K. Porteous, E.C. Ledgerwood, R.A. Smith, M.P. Murphy, Selective targeting of a redox-active ubiquinone to mitochondria within cells: antioxidant and antiapoptotic properties, J Biol Chem, 276 (2001) 4588-4596.

[21] Y. Yamada, H. Akita, H. Harashima, Multifunctional envelope-type nano device (MEND) for organelle targeting via a stepwise membrane fusion process, Methods Enzymol, 509 (2012) 301-326.
[22] S. Haga, S.J. Remington, N. Morita, K. Terui, M. Ozaki, Hepatic ischemia induced immediate oxidative stress after reperfusion and determined the severity of the reperfusion-induced damage, Antioxid Redox Signal, 11 (2009) 2563-2572.
[23] Y. Shinohara, M.R. Almofti, T. Yamamoto, T. Ishida, F. Kita, H. Kanzaki, M. Ohnishi, K. Yamashita, S. Shimizu, H. Terada, Permeability transition-independent release of mitochondrial cytochrome c induced by valinomycin, Eur J Biochem, 269 (2002) 5224-5230.
[24] J. Snoeys, J. Lievens, E. Wisse, F. Jacobs, H. Duimel, D. Collen, P. Frederik, B. De Geest, Species differences in transgene DNA uptake in hepatocytes after adenoviral transfer correlate with the size of endothelial fenestrae, Gene Ther, 14 (2007) 604-612.
[25] I.A. Khalil, Y. Hayashi, R. Mizuno, H. Harashima, Octaarginine- and pH sensitive fusogenic peptide-modified nanoparticles for liver gene delivery, J Control Release, 156 (2011) 374-380.
[26] D. Mudhakir, H. Akita, K.I. A., S. Futaki, H. Harashima, Pharmacokinetic analysis of the tissue distribution of octaarginine modified liposomes in mice, Drug Metab Pharmacokinet, 20 (2005) 275-281.
[27] Y. Hayashi, J. Yamauchi, I.A. Khalil, K. Kajimoto, H. Akita, H. Harashima, Cell penetrating peptide-mediated systemic siRNA delivery to the liver, Int J Pharm, 419 (2011) 308-313.
[28] E. Wisse, F. Jacobs, B. Topal, P. Frederik, B. De Geest, The size of endothelial fenestrae in human liver sinusoids: implications for hepatocyte-directed gene transfer, Gene Ther, 15 (2008) 1193-1199.
[29] A.L. Klibanov, K. Maruyama, A.M. Beckerleg, V.P. Torchilin, L. Huang, Activity of amphipathic poly(ethylene glycol) 5000 to prolong the circulation time of liposomes depends on the liposome size and is unfavorable for immunoliposome binding to target, Biochim Biophys Acta, 1062 (1991) 142-148.
[30] D. Liu, A. Mori, L. Huang, Role of liposome size and RES blockade in controlling biodistribution and tumor uptake of GM1-containing liposomes, Biochim Biophys Acta, 1104 (1992) 95-101.
[31] S. Greenberg, W.H. Frishman, Co-enzyme Q10: a new drug for cardiovascular disease, J Clin Pharmacol, 30 (1990) 596-608.
[32] D.V. Ratnam, D.D. Ankola, V. Bhardwaj, D.K. Sahana, M.N. Kumar, Role of antioxidants in prophylaxis and therapy: A pharmaceutical perspective, J Control Release, 113 (2006) 189-207.
[33] Y. Sato, H. Mutoh, M. Suzuki, Y. Takekuma, K. Iseki, M. Sugawara, Emulsification Using Highly Hydrophilic Surfactants Improves the Absorption of Orally Administered Coenzyme Q10, Biological & Pharmaceutical Bulletin, 36 (2013) 2012-2017.
[34] M.J. McManus, M.P. Murphy, J.L. Franklin, The mitochondria-targeted antioxidant MitoQ prevents loss of spatial memory retention and early neuropathology in a transgenic mouse model of Alzheimer's disease, J Neurosci, 31 (2011) 15703-15715.
[35] J.R. Mercer, E. Yu, N. Figg, K.K. Cheng, T.A. Prime, J.L. Griffin, M. Masoodi, A. Vidal-Puig, M.P. Murphy, M.R. Bennett, The mitochondria-targeted antioxidant MitoQ decreases features of the metabolic syndrome in ATM+/-/ApoE-/- mice, Free Radic Biol Med, 52 (2012) 841-849.
[36] R.A. Smith, M.P. Murphy, Animal and human studies with the mitochondria-targeted antioxidant MitoQ, Ann N Y Acad Sci, 1201 (2010) 96-103.
[37] E.J. Gane, F. Weilert, D.W. Orr, G.F. Keogh, M. Gibson, M.M. Lockhart, C.M. Frampton, K.M. Taylor, R.A. Smith, M.P. Murphy, The mitochondria-targeted anti-oxidant mitoquinone decreases liver damage in a phase II study of hepatitis C patients, Liver Int, 30 (2010) 1019-1026.
[38] B.J. Snow, F.L. Rolfe, M.M. Lockhart, C.M. Frampton, J.D. O'Sullivan, V. Fung, R.A. Smith, M.P. Murphy, K.M. Taylor, G. Protect Study, A double-blind, placebo-controlled study to assess the mitochondria-targeted antioxidant MitoQ as a disease-modifying therapy in Parkinson's disease, Mov Disord, 25 (2010) 1670-1674.
[39] V.J. Adlam, J.C. Harrison, C.M. Porteous, A.M. James, R.A. Smith, M.P. Murphy, I.A. Sammut, Targeting an antioxidant to mitochondria decreases cardiac ischemia-reperfusion injury, FASEB J, 19 (2005) 1088-1095.
[40] J. Neuzil, C. Widen, N. Gellert, E. Swettenham, R. Zobalova, L.F. Dong, X.F. Wang, C. Lidebjer, H. Dalen, J.P. Headrick, P.K. Witting, Mitochondria transmit apoptosis signalling in cardiomyocyte-like

cells and isolated hearts exposed to experimental ischemia-reperfusion injury, Redox Rep, 12 (2007) 148-162.

SUPPLEMENTARY MATERIAL

Supplementary Methods

1. Isolation of mitochondria from mouse livers

Mitochondria were isolated from livers obtained from C57BL/6 male mice (6 weeks of age). Mice were sacrificed, and the livers were removed after the bleeding was performed with a heparin solution (40 U/mL), which was then collected and washed with saline. All subsequent steps were carried out on ice. After removing the saline, the livers were placed in 3 mL of ice-cold mitochondrial isolation buffer [MIB: 250mM sucrose, 2 mM Tris–HCl, 1 mM EDTA, pH 7.4], and were then minced with scissors and ice-cold MIB (+) was added to a total volume of 9 mL. The suspension homogenized in a glass homogenizer (30 mL capacity) with a pestle using 3 complete up and down cycles (~ 550 rpm). The homogenate was mixed with approximately 1 mL of MIB (+) and centrifuged at 800*g* for 5 min. The supernatant was transferred into ice-cold tubes and centrifuged at 7,500*g* for 10 min. The pellets were washed twice with EDTA-free MIB and reprecipitated by centrifugation (16,000*g*, 10 min), and the pellets were resuspended with EDTA-free MIB and the resulting suspensions were used as the isolated mitochondrial suspension. Protein concentrations of mitochondrial proteins were determined using a BCA protein assay kit (Pierce, Rockford, IL).

2. Estimation of encapsulation efficiency of the CoQ_{10} into MITO-Porter.

To estimate encapsulation efficiency, a CoQ_{10}-MITO-Porter (DOPE/SM/STR-R8/DMG-PEG2000/CoQ_{10} [9/2/0.33/0.33/1.8]) containing a lipid film labeled with DiI (0.5 mol% of total lipids) was prepared using the ethanol dilution method as described in Materials and methods of the main text. The CoQ_{10}-MITO-Porter was separated from the unentrapped CoQ_{10} by ultrafiltration through an Amicon system, and the recovered CoQ_{10} and the recovered lipids were then determined after treatment with SDS (final concentration, 1%). The applied CoQ_{10} and the applied lipids were also determined before removing the ethanol by ultrafiltration. The amounts of CoQ_{10} were determined by measuring the absorbance at 275 nm. The amounts of lipid were determined by measuring the fluorescent intensity of the DiI (excitation at 560 nm and emission at 590 nm). The encapsulation efficiency was calculated using equation shown below:

encapsulation efficiency (%) = (recovered CoQ_{10} / recovered lipid)/ (applied CoQ_{10} / applied lipid) x 100.

3. Western blotting analysis

The sample (2 μg protein of mitoplast suspension /μL) was heated (95°C, 5 min) with an equal of loading buffer (100 mM Tris-HCl (pH 6.8), 4% SDS, 12% 2-mercaptoethanol, 20% glycerol, 0.05% bromophenol blue), and then subjected to 15% SDS-PAGE. After electrophoresis, the proteins were electroblotted onto a Polyvinylidene Fluoride membrane (NIPPON Genetics Co., Ltd; Tokyo, Japan) and the membranes were then blocked with 5% nonfat dry milk. After blocking, primary antibodies from the mouse against the COX IV (Abcam; Cambridge, UK), rabbit against Histone H3 (Merck Millipore; Billerica, MA, USA) and rabbit against GAPDH (Cell signaling Technology; Danvers, MA, USA), as mitochondrial, nuclear and cytosolic fraction markers, were used at dilutions of 1:10,000, 1:2,000, and 1:3,000, respectively. These proteins were detected using secondary HRP-conjugated anti-rabbit at 1: 1000 dilution or anti-mouse antibodies at 1: 2000 dilution (GE Healthcare UK Ltd, Buckinghamshire, England). Blots were developed with Amersham ECL Plus Western Blotting Detection System (GE Healthcare). Immunoreactive bands were visualized using LAS 4000 (Fujifilm, Tokyo, Japan).

4. Investigation of the stability of the CoQ_{10}-MITO-Porter in serum.

A 100 μL aliquot of the CoQ_{10}-MITO-Porter (DOPE/SM/STR-R8/DMG-PEG2000/CoQ_{10} [9/2/0.33/0.33/1.8], 0.2 mM lipids) suspension was mixed with an equal volume of fetal bovine serum (Invitrogen Corp, Carlsbad, CA) or HEPES buffer in a tube, and the resulting suspension was then incubated at 37°C with shaking (800 rpm) using a shaking incubator (SI-300C, AS ONE, Osaka, Japan). After the incubation, the size distributions of the carriers were measured using a dynamic light scattering method (Zetasizer Nano ZS), and the values for the main peak are shown in Figure S3.

Supplementary Figures

Figure S1. Quantification of carrier accumulation in liver mitochondria by RI.

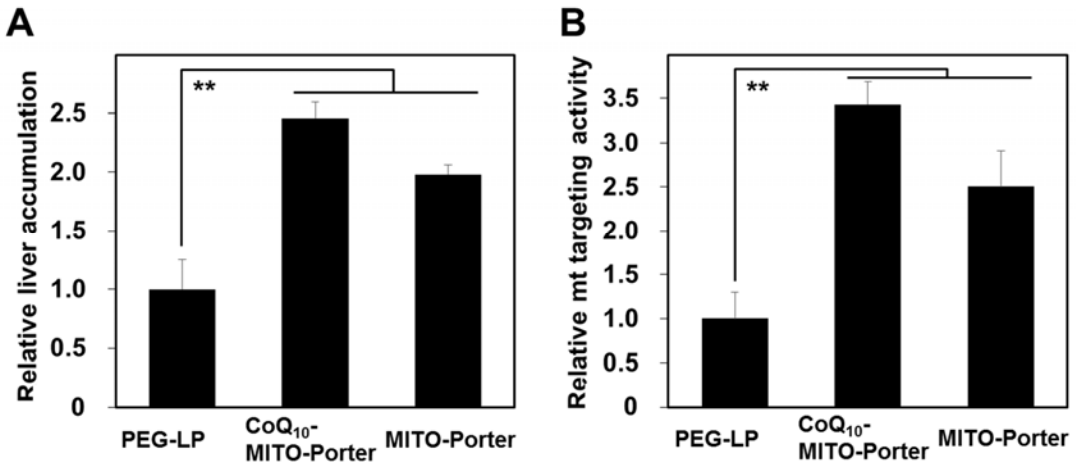

PEG-LP, CoQ_{10}-MITO-Porter (3 mol% of R8) and MITO-Porter labeled with [^{3}H]-CHE were systemically injected into the tail vein of mice. The values for relative liver accumulation (**A**) and relative mitochondrial targeting activity (**B**) were calculated from the count of [^{3}H] in the liver and mitochondrial lysate 1 hr after injection. Bars indicate means ± S.D. (n=3-5). **Significant differences ($p<0.01$) between PEG-LP and others were calculated by one-way ANOVA, followed by Bonferroni test.

Figure S2. Evaluation of therapeutic effect of MitoQ.

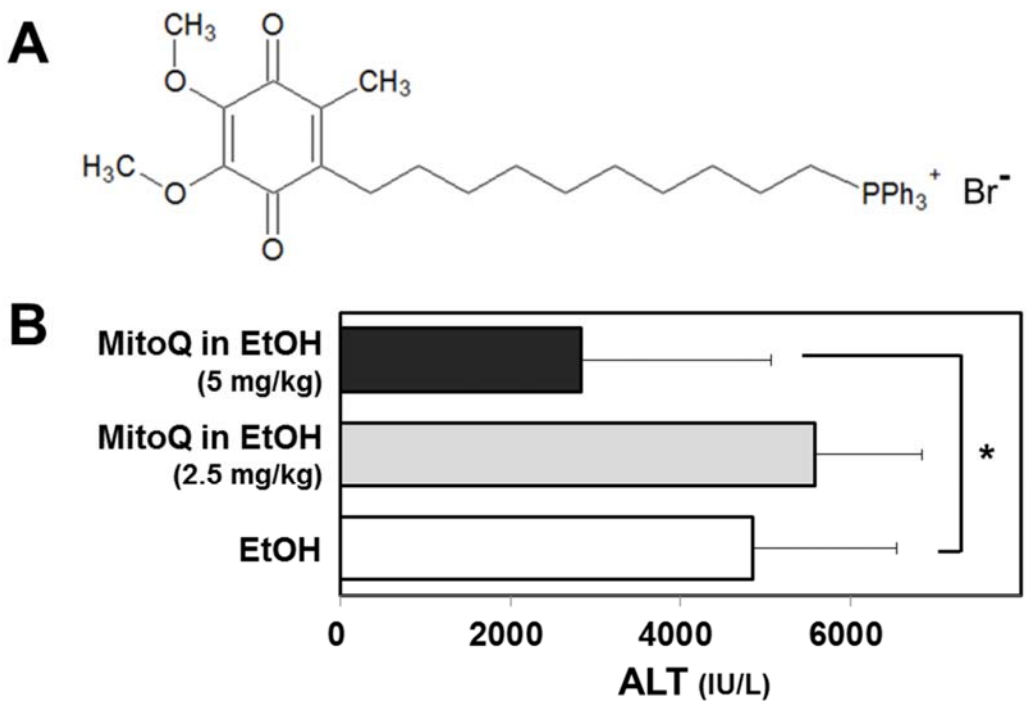

(**A**) Chemical structure of MitoQ. (**B**) Evaluation of hepatoprotective effect from I/R injury. MitoQ was administered into mice via intraperitoneal injection at a dose of 2.5 and 5 mg MitoQ/kg body weight. Serum ALT activities were measured at 6hr after the I/R injury. Data are represented as the mean ± S.D. (n = 4-9). *Significant difference between EtOH and others ($p < 0.05$ by one-way ANOVA, followed by Bonferroni test).

Figure S3. Investigation of the stability of the CoQ_{10}-MITO-Porter in serum.

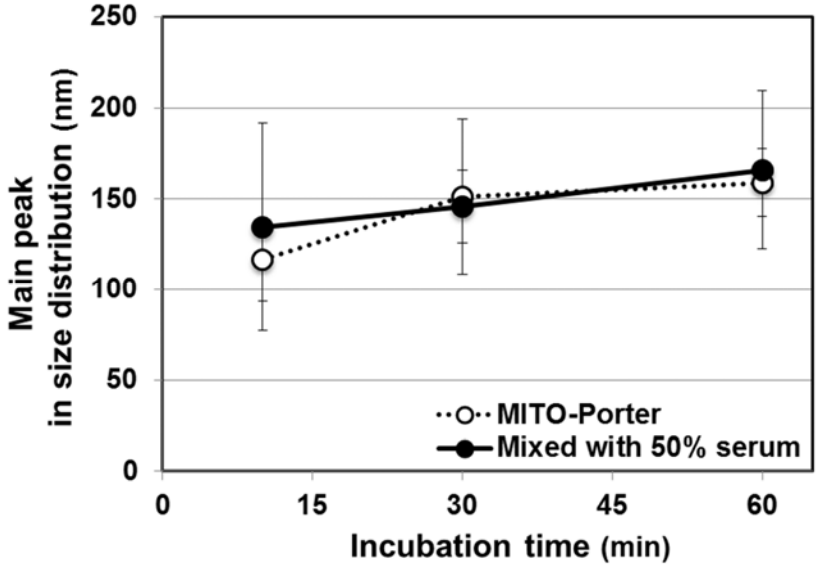

The CoQ_{10}-MITO-Porter was mixed with serum (closed circles) or HEPES buffer (open circles) and incubated at 37°C with shaking for various times (10, 30, 60 min). After the incubation, the diameters of the carriers were measured. Data denote the mean ± S.D. (n=4).

Figure S4. Biodistribution of the CoQ_{10}-MITO-Porter.

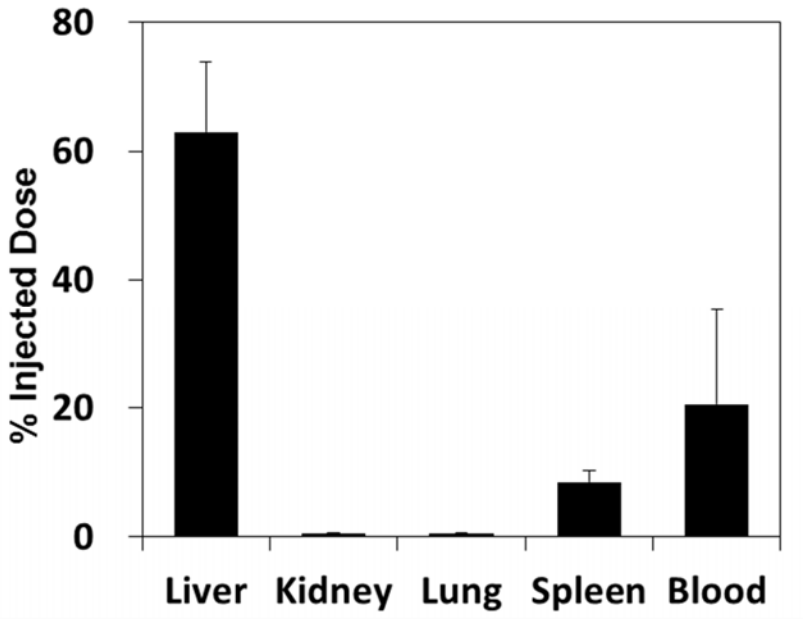

CoQ_{10}-MITO-Porter (10 mol% of R8) labeled with [^{3}H]-CHE were systemically injected into the tail vein of mice. Tissue distribution was analyzed from the count of [^{3}H] in the tissue lysate at 30 min after the injection. Bars indicate means ± S.D. (n=3).

Supplementary Table

Table S1. Characteristics of the carriers prepared by hydration methods.

	Compositions [molar ratio]	Diameters (nm)	ζ-potentials (mV)
MITO-Porter	DOPE/SM/STR-R8 [9/2/1.1]	197±31	50±3
PEG-LP	DOPE/SM/DMG-PEG2000 [9/2/0.33]	95±3	-4.6±1.6

Carriers labeled with 0.5 mol% DiI were used for histological observation of the carriers in the liver. Data are means ± S.D. (n=3). DOPE, 1,2-dioleoyl-sn-glycero-3-phosphatidylethanolamine; SM, sphingomyelin; DMG-PEG 2000, 1,2-dimyristoyl-sn-glycerol, methoxypolyethylene glycol 2000; STR-R8, stearylated octaarginine.

Table S2. Characteristics of carriers with low fusogenic activities prepared for binding and fusion assays.

Carriers-type	[a]Liposomes for biding assay			[b]Liposomes for fusogenic assay		
	Size (nm)	PDI	ζ-potential (mV)	Size (nm)	PDI	ζ-potential (mV)
CoQ_{10}-EPC-LP	43±2	0.33±0.01	-5.7±3.2	45±2	0.36±0.01	-5.9±1.3
CoQ_{10}-R8-EPC-LP	43±1	0.35±0.02	18±2	46±1	0.38±0.02	18±3

[a]Liposomes labeled with 1 mol% NBD–DOPE were used for biding assay

[b]Liposomes labeled with both 1 mol% NBD–DOPE and 0.5 mol% rhodamine–DOPE were used for fusion assay. Data are means ± S.D. (n=3).